Effects of gravel layer as thrust restraint for pipe bends subjected to earthquake loading

Ohta, Yoko
Sawada, Yutaka
Ariyoshi, Mitsuru
Mohri, Yoshiyuki
Kawabata, Toshinori

(Citation)
International Journal of Physical Modelling in Geotechnics,22(2):99-110

(Issue Date)
2021-03-11

(Resource Type)
journal article

(Version)
Accepted Manuscript

Effects of gravel layer as thrust restraint for pipe bends subjected to earthquake loading

Author 1

- Yoko OHTA, Student
- Graduate School of Agricultural Science, Kobe University, Kobe, Japan
- 0000-0003-4208-1518

Author 2

- Yutaka SAWADA, Associate Professor
- Graduate School of Agricultural Science, Kobe University, Kobe, Japan
- 0000-0001-5517-3345

Author 3

- Mitsuru ARIYOSHI, Senior Researcher
- Division of Facilities and Geotechnical Engineering, Institute for Rural Engineering, Tsukuba, Japan

Author 4

- Yoshiyuki MOHRI, Professor
- Faculty of Agriculture, Ibaraki University, Inashiki, Japan

Author 5

- Toshinori KAWABATA, Professor
- Graduate School of Agricultural Science, Kobe University, Kobe, Japan

Full contact details of corresponding author.

Yutaka SAWADA

1-1, Rokkodai-cho, Nada-ku, Kobe, 657-8501, JAPAN

Lab. of Geotechnical Engineering for Agriculture

Graduate school of Agricultural Science

Kobe University

Phone: +81 78 803 5902

E-mail: sawa@harbor.kobe-u.ac.jp

Written on 14/09/2020

Number of words in the main text (excluding abstract and references): 4786

Number of figures and tables: 13 figures, 2 tables

Abstract

This paper reports effects of gravel layers as a thrust restraint in a pipe bend subjected to earthquake loading based on the shaking table tests in a centrifuge. The model pipe was buried under four backfill conditions differing in the existence and layout of a gravel layer. The pipe was pulled laterally with a constant load, simulating the thrust force generated at bends in generally pressure pipelines with diameters of 1800 mm. Shakings were conducted on the model pipe with lateral loading. The test results showed that the gravel surrounding the pipe was effective as a thrust restraint for pipes of large diameter. A gravel layer on the passive side was found to be particularly crucial. A gravel layer on the active side provided no thrust restraint effect, although it did reduce pipe displacement amplitude. A gravel layer on the upper half of the passive side of the pipe likely contributed to mitigation not only of lateral displacement but also of pipe uplift.

Keywords chosen from ICE Publishing list
Pipes & pipelines; Earthquakes; Pore pressures

List of notations

D	outer diameter of the pipe
E_1	axial displacement
E_2	axial displacement caused by the angular displacement
g	acceleration due to gravity
H	depth of embedment of the pipe
h	depth of the earth cover
L	length of the straight pipe
$v(t)$	velocity at time t
α	separation between the pipe bend and the straight pipe in the axial direction
γ_{sat}	unit weight of the saturated sand
γ_w	unit weight of water
Δu	excess pore water pressure
δ	displacement of the pipe bend
θ	bending angle of the pipe bend
ρ_s	density of soil particles
ϕ	angular displacement

1. Introduction

Seismic damage to pressure pipelines concentrates at pipe bends, in particular the separation of joints due to the lateral displacement of bends. Harumoto *et al*. (2015) reported that about 25% of the pipeline damage occurred at bends during the 2011 off the Pacific coast of Tohoku Earthquake. At a bend in a pressure pipeline, unbalanced thrust force is generated by the internal pressure, as shown in Figure 1. According to the design guidelines, the passive resistance of soil resists the thrust force (MAFF, 2009; AWWA, 2013). When such resistance is insufficient to prevent movement of the pipe, a concrete block can be used to increase the passive resistance and the frictional force. However, if the surrounding soil is liquefied, then the concrete block becomes a weak point because of its heavy weight. The heavy block leads to not only the sinking of pipes but also the lateral movement of pipes during earthquakes due to inertia force.

Many researchers have taken interest in the lateral movement of pipes in soil. Experimental studies have been conducted using straight pipes under ordinary gravitational conditions of 1 g to obtain the relationship between the resistance force and the lateral displacement (Audibert and Nyman, 1977; Trautmann and O'Rourke, 1985; Hsu, 1993). In recent years, numerical analyses using the Distinct Element Method and Finite Element (FE) Method have been carried out to investigate pipe-soil interaction in a plane strain condition (Yumsiri and Soga, 2006; Kouretzis *et al*., 2013; Roy *et al*., 2018). Daiyan *et al*. (2011) conducted lateral loading experiments in various loading directions under a centrifugal acceleration of 12.3 g and also carried out 3D FE analysis. The results showed that when the oblique angle was greater than 40^{o}, the failure mechanism of the soil around the pipe changed and the axial resistance which related to the friction on the pipe surface decreased. In research on pipe bends, Cheong *et al*. (2011) conducted 3D FE analysis to evaluate the normal force acting on a pipe bend considering pipe deformation. The numerical results indicated that the soil force against the elbow section was higher than that against the straight section because soil deformation was concentrated on the elbow section. Huang *et al*. (2020) performed shaking table tests and numerical analyses on pipelines including bends and proposed an equation of normal earth pressure at the pipe bend based on the normal earth pressure on the straight pipe. Despite this

plentiful research on the lateral displacement of pipes, experimental study remains limited for large-diameter pipes, such as agricultural pipes, which can reach 1000 mm in diameter.

In a study on thrust restraint methods as alternatives to concrete blocks, Fujita *et al*. (2007) conducted experiments and numerical analyses to examine the stability of straight pipes which were installed in a curved alignment. This method diminishes the thrust force acting on a pipe compared with that acting on a pipe bend, but the arrangement requires a large site for construction. Therefore, the curved arrangement can apply only to a limited subset of potential sites. Itani *et al*. (2016) carried out the shaking table tests for the chain-structure pipelines confirming the effectiveness of the chain structure against the displacement of the pipe bends during earthquakes. Such a chain structure is sufficient for mitigating seismic damage of pipelines, but the construction of such structure is expensive.

As a new inexpensive method that can be applied anywhere, the thrust restraint using gravel and a geogrid has been proposed. Ohta *et al*. (2018-b, 2019) performed lateral loading experiments and shaking table tests to evaluate the effectiveness of thrust restraint using gravel and a geogrid. Their experimental results implied that gravel was useful for preventing pipe moving during liquefaction. Meanwhile, the purchase of good quality gravel can be costly. Therefore, a recommended minimum amount of gravel is necessary for reasonable design.

In this study, shaking table tests were conducted on buried pipes under a 30 g gravitational field for the purpose of examining the effective layout of gravel backfill for the stability of large-diameter pipes subjected to the thrust force under earthquake loading.

2. Outline of experiments

As mentioned in the Introduction, the aim of the tests was to investigate the effective layout of gravel backfill as a thrust restraint during an earthquake. Figure 2 shows the test conditions for the four tests reported in this paper. The tests differed solely in gravel installation layout. A series of shaking table tests was performed under 30 g at a corresponding length scale factor of 1:30. These tests facilitated the observation of the seismic behaviour of a pipe representing a

prototype diameter of 1800 mm. The centrifuge scaling laws for these tests are shown in Table 1.

2.1 Test equipment

The centrifugal model tests were conducted using a geotechnical beam centrifuge equipped with a seismic shaker at the National Agricultural and Food Research Organization in Japan. The beam centrifuge, of radius 4.8 m, can reach a maximum centrifugal acceleration of 75 g during dynamic tests. The maximum carrying mass is 3000 kg. The seismic shaker on the centrifuge is 1000 mm in length and 1500 mm in width. The shaker can perform a maximum shaking acceleration of 55 g. Available shaking frequencies range from 10 to 400 Hz.

The dimensions of the rigid test container (Figure 3) were 1350 × 400 × 450 mm. The front face of the testing container was a transparent window, while the side walls and the back wall were made of steel. Valves were installed on the bottom of the container to allow fluid to be supplied to the model ground under the centrifugal field. Details of the saturation process are described in subsection 2.4.

Thrust force was simulated by the lateral load. The loading system, as shown in Figure 4, consisted of a wire, a weight and pulleys to apply a constant load laterally to the model pipe during experiments. The masses of the weights were set to 7 or 14 kg. The lateral loads on the prototype scale corresponded to full-scale thrust forces under internal pressures of 150 or 300 kPa. These internal pressures were calculated assuming that the full-scale pipe bend has an outer diameter of 1800 mm and a bending angle of 45°. Note that the internal pressure of 150 kPa is a typical pressure for agricultural pipelines in Japan.

The aluminium model pipe is shown in Figure 4(b). Although the thrust force is actually generated at the pipe bend, a straight pipe was used in the present experiments. Ohta *et al.* (2018-a) conducted the lateral loading experiments for three model pipes which had different bending angles but the same projected length. The results showed that the bending angle of pipes hardly affected the lateral resistance. Additionally, the centrifugal tests had limitations of

choice of the test container. Therefore, we conducted the experiments under two-dimensional condition. The outer diameter, length and mass of the model pipe were 60 mm, 396 mm and 2.3 kg, respectively. Both ends of the pipe were closed. A sponge was putted on the two ends of pipe along the edges to prevent soil from flowing into gaps between the pipe ends and the container walls. The friction between the sponge and the container wall was reduced by fluorine coating. The unit weight of the model pipe was approached that of the model ground in order to avoid the uplifting and sinking of the model pipe during experiments. The unit weights of the model pipe and the saturated silica sand were 20.5 kN/m^3 and 19.5 kN/m^3, respectively. The model pipe was pulled laterally by the wire through the centre of the model pipe. The wire (ϕ4) passed through an aluminium tube (ϕ6) buried in the model ground to decrease friction between the wire and soil.

2.2 Soil properties and model preparation

The model grounds were prepared using three kinds of soil to simulate the natural ground and the backfill ground, respectively. In most real-world cases, the backfill ground is easier to liquefy than the natural ground. Therefore, in this study, the backfilled ground and the natural ground were simulated separately using soils with different liquefied strength.

Well-graded sand, called Kasama sand in Japan, was used to reproduce the natural ground. Well-graded sand is classified as SF. This soil was selected to reduce the saturation time. The natural ground did not liquefy during experiments, as shown in subsection 3.1. The dry unit weight of the well-graded sand was 13.8 kN/m^3, which was 93% of the maximum dry weight on the basis of a standard Proctor compaction test. The initial void ratio of the sand was 0.84. Silica sand and gravel were used to reproduce the backfill ground. The dry unit weights of silica sand and gravel were 15.6 kN/m^3 and 16.2 kN/m^3, respectively. The initial void ratio of silica sand and gravel were both 0.66. The unit weight of silica sand corresponded to a relative density of 60%. Note that the maximum and minimum dry densities of silica sand were 17.2 kN/m^3 and 13.7 kN/m^3, respectively. Densities of silica sand and gravel were determined based on the results of cyclic undrained triaxial tests described later. The particle sizes and physical properties of the ground materials are shown in Figure 5.

Klinkvort et al. (2018) summarised the results of previous studies and reported that no scale effect on the lateral load of a model pile was observed when the ratio of pile diameter and D_{50} (the average grain size) was greater than 40, 60 or 88. Gravel in our experiments was too large to avoid the scale effect because the ratio of the pipe diameter and D_{50} of gravel is 18. To ignore the scale effect, D_{50} of a backfill material have to be less than 1.5 mm. Ono *et al.* (2019) showed that the layers made of the soil with D_{50} of about 1.5 mm were liquefied during shaking (i.e. excess pore water pressure = 1.0). The result does not correspond to the well-known fact that the layer made with gravel (maximum particle size of 25~40mm) hardly liquefied in the real field. Selection of the material which meets both requirements of the bearing capacity and the permeability is impossible. Gravel with D_{50} of 3.29 mm was chosen in the experiments to ensure the dissipation of the excess pore water pressure, which was the important characteristic of gravel.

The cyclic undrained triaxial tests were performed on silica sand and gravel. In the triaxial tests, specimen densities were the same as in the centrifugal tests. A confining pressure of 35 kN/m^2 was applied to each specimen. This confining pressure was nearly equal to the effective confining pressure at the spring line of the pipe. The results of the cyclic undrained triaxial tests are shown in Figure 6. Based on the results in Figure 6(a), the liquefied strength ratios of silica sand and gravel were 0.42 and 1.12, respectively. Although the liquefied strength of silica sand was slightly high for reproducing a liquefied ground, this density was adopted in the experiments as a means of considering the condition of sand ground *in situ*. Note that the liquefied strength was determined by the cyclic stress ratio at a cycle number of 20 and a double-amplitude axial strain of 5%.

The following describes the preparing procedure of the model ground. Before preparing the ground, a filter of 10 mm thickness was set on the bottom of the test container. The filter was made of gravel with an average grain size of 3.29 mm. A nonwoven fabric covered the surface of the filter in order to protect the soil from running out into the filter layer. The natural ground was prepared on the filter. The well-graded soil was compacted in 13 layers (10~20 mm per

layer). The water content of the well-graded soil was adjusted to 24%, which is the optimum moisture content for easing compaction. After the natural ground was compacted, a trench was excavated, and the model pipe was buried with gravel and silica sand as shown in Figure 2. The backfill ground was compacted in 10 layers (10~20 mm per layer). The water content of the silica sand was adjusted to 5%. When the model ground was completed, the test container was mounted on the centrifuge shaker. The saturation process was conducted under centrifugal field of 30 g.

2.3 Test conditions

Four different types of backfilling conditions were investigated in this study, as shown in Figure 2. The dimensions of the trench were determined on the basis of the design guidelines in Japan (MAFF, 2009). The depth of the trench was 160 mm (H/D = 1.5), where 1.5 is the typical ratio for large-diameter pipes. The gradients of both slopes were 1:0.6. The width of the trench at the bottom of the pipe was 120 mm. The thickness of the bedding under the pipe was 10 mm.

In case A, the pipe was backfilled only with silica sand. In case B, a gravel layer extended upwards from the bottom of the trench to the top of the pipe. The amounts of gravel used in cases C and D were approximately half that of case B in order to assess the effects of the amount and arrangement of gravel in thrust restraint. In case C, gravel was placed up to the height of the spring line as shown in Figure 2. The resistance acting on the lower half of the pipe was important in resisting pipe displacement. Kawabata *et al*. (2002) pointed out that the passive horizontal earth pressure distribution acting on the pipe experiences a peak at about 45° below the spring line for a laterally loaded pipe. Therefore, if the ground on the lower half of the pipe is not liquefied, the lateral resistance might be maintained sufficiently. On the other hand, Palmer *et al*. (2009) mentioned that the vertical force at the lower leading quarter of the pipe causes the uplifting of the pipe. Reinforcing only the ground on the bottom half of the pipe might therefore risk uplifting of the pipe. In case D, only the passive side of the pipe was backfilled with gravel. Needless to say, passive resistance is important in thrust restraint. The pipe in case D was expected to experience the same resistance force as in case B because cases B and D had the same amount of gravel on the passive side of the pipe. On the other

hand, if the soil on the active side of the pipe were to liquefy, then the pipe could move substantially to the active side under seismic conditions. In other words, the displacement amplitude of the pipe could become large and affect the stability of the buried pipe.

2.4 Experimental procedure

Shaking tests in all cases were carried out with a loading mass of 7 kg initially to assess the effectiveness of the gravel layer as the thrust restraint. After preparing the model ground, the testing container was placed on the centrifuge, and a mass of 7 kg was installed. The saturation process was performed under a centrifugal field of 30 g. In the saturation process, a viscous liquid made of Metolose was used. The viscosity of the fluid was adjusted to 30 times that of water in order to reduce the permeability of the sand, thereby reproducing the desired pore pressure response of water under the centrifugal field. The centrifuge was equipped with a rotary joint so that the liquid was provided from the outside during each run. Pressurised fluid was introduced to the model ground slowly from the bottom of the model ground under a centrifugal field of 30 g. Each saturation process was performed gradually over the course of more than 12 hours to avoid the occurrence of air bubbles in the model ground.

After shaking under a loading mass of 7 kg, the centrifuge was stopped, and the loading mass was increased to 14 kg. In cases C and D, the shaking process was then conducted again. The mass was increased to 14 kg because a loading mass of 7 kg produced no displacement difference between cases C and D. A difference in results between cases C and D under a loading of 14 kg was observed, and the gravel layer's effects on pipe behaviour were investigated. Note that displacement of the pipe due to the change of lateral load from 7 to 14 kg was rarely observed.

In the shaking process, four shaking regimes with prototype accelerations of 2, 4, 6 and 8 m/s^2 were applied to the models. The prototype frequency and duration of the shaking were 5 Hz and 60 s, respectively. Acceleration responses of the shaking table are shown in Figure 7. The shaking interval had sufficient time to dissipate excess pore water pressure in the model ground. To judge the level of shaking applied to the test models, the Power Spectral Intensity (PSI) was

calculated. The PSI value, proposed by Nozu and Iai (2001), indicates the intensity of an earthquake. Nozu and Iai (2001) pointed out that the PSI value has a higher correlation with seismic damage to structures than does the maximum acceleration. The PSI value was calculated using the following equation.

$$PSI = \left(\int_0^{\infty} \left(v(t)^2 \right) dt \right)^{0.5}$$

1.

The calculated PSI values for the prototypes are shown in Table 2. PSI values for the 2011 off the Pacific coast of Tohoku Earthquake are also calculated for comparison. The calculated results imply that the level of shaking at 8 m/s^2 (PSI of 133) was almost the same as that of the 2011 Tohoku earthquake (PSI of 130). The shaking condition of this experiment was therefore quite severe.

3. Results

All experimental results are presented at the prototype scale.

3.1 Response of excess pore water pressure ratio

Figure 8 shows the response of the excess pore water pressure ratio (EPWPR) in cases A and B. The EPWPR is defined as the measured excess pore water pressure divided by the initial effective overburden pressure at the depth of the pore pressure transducers, as shown in Equation 2. The actual initial effective stress in the model ground was different from the simple overburden pressure due to the effects of the trench and the pipe. Therefore, the value of EPWPR calculated from Equation 2 is used only as a guide.

$$\mathrm{EPWPR} = \frac{\Delta u}{(\gamma_{\mathrm{sat}} - \gamma_{\mathrm{w}}) \cdot h}$$

2.

In case A, in which the pipe was backfilled with only silica sand, the EPWPR in the backfill ground rose to around 0.6, while the EPWPR in the natural ground barely increased. The

difference in liquefaction properties between the backfill ground and the natural ground manifested clearly.

In case B, in which the pipe was backfilled with gravel and silica sand, the pore water pressure accumulated less than in case A because gravel was able to dissipate the excess pore pressure rapidly. The large amplitude of the pore water pressure in gravel as shown in Figure 8 is the typical shear behaviour of gravel under undrained conditions. A similar behaviour is confirmed for gravel in Figure 6(b, c), which shows the responses of gravel and silica sand during the cyclic loading tests described in subsection 2.2.

3.2 Pipes after experiments

Figure 9(a, b) shows images of the test models after shaking at a maximum acceleration of 8 m/s^2. Yellow crosses in the images denote the positions of the pipe centres after each shaking. As shown in Figure 9(a), the pipe without gravel (case A) moved substantially, whereas the pipes with gravel (cases B, C and D) moved only slightly.

Focussing on pipe behaviour, the pipe in case A displaced drastically not only laterally but also upwards. Ono *et al*. (2016) reported pipe uplift associated with lateral displacement in liquefied ground when the pipe moved along the slope of the failure surface as suggested by Audibert and Nyman (1977). Note that the unit weight of the model pipe in this study was adjusted to that of the saturated silica sand to avoid buoyancy-related uplift of the pipe. As for the cases with gravel, the pipe in case C uplifted at a loading mass of 14 kg, whereas the pipe in case D seemed to move only laterally during shaking. The relationship between the gravel layer layout and the uplift of the pipe is further discussed in subsection 4.4.

Focussing on the behaviour of the gravel layer, the gravel layer on the passive side seemed to be compressed by the pipe. However, the shape of the layer did not deform drastically, except in case C at a loading mass of 14 kg.

3.3 Lateral displacement of pipes

Figure 10(a, b) shows the lateral displacement of the pipe as measured by a laser displacement transducer. The lateral displacement values for the pipe in Figure 10 are normalised by the outer diameter of the model pipe. The dotted line in Figure 10 represents the normalised displacement limit at which a pipe with ϕ1800 is able to maintain function. The displacement limit is determined by the displacement of the pipe bend when an angular displacement ϕ or a sum of E_1 and E_2 (see Figure 11) reaches its allowable value. The allowable values of ϕ and E_1 +E_2 were set to 5° and 168 mm, respectively, referring to FRP pipe standards. ϕ, E_1 and E_2 were calculated using Equation 3, quoted from Itani *et al*. (2016).

$$E_1 = \frac{\alpha}{2} - \frac{D}{2} \times \sin\phi$$

$$E_2 = D \times \sin\phi$$

$$\alpha = \sqrt{\left(L + \delta \times \sin\frac{\theta}{2}\right)^2 + \left(\delta \times \cos\frac{\theta}{2}\right)^2} - L$$

$$\phi = \cos^{-1}\left(\frac{L + \delta \times \sin\frac{\theta}{2}}{L + \alpha}\right)$$

3.

The displacement limit was calculated based on the following assumptions: D = 1800 mm, θ = 45° and L = 4000 mm. When the displacement of the pipe bend δ was 393 mm, the corresponding values of φ and E_1+ E_2 were 5° and 162 mm, respectively. Therefore, the displacement limit of the pipe bend was determined to be 393 mm, representing a normalised value of 0.22.

4. Discussion

The effectiveness of gravel backfill was assessed mainly in terms of the lateral displacement of the pipe during shaking. The effectiveness of gravel for mitigating pipe uplift is also discussed because pipe uplift also causes damage to pipes.

4.1 Effectiveness of gravel backfill as thrust restraint

The effectiveness of a gravel layer as a thrust restraint (Figure 10 (a)) was examined. In case A without gravel, the pipe displaced far beyond the displacement limit at a shaking acceleration of 4 m/s^2 (PSI of 66), while in the cases with gravel, the pipe displaced within the displacement limit even at a shaking acceleration of 8 m/s^2 (PSI of 133). These results show that backfilling the pipe with gravel is effective in the preventing of the displacement of large-diameter pipes subjected to thrust force during large earthquakes.

4.2 Effects of gravel on the passive side of a pipe

Regarding the layout of gravel backfill, there was little difference among the lateral displacement responses in cases B, C and D during shaking (loading mass = 7 kg), as shown in Figure 10(a). These results imply that a small amount of gravel, as used in case C or D, is sufficient for thrust restraint to counter typical thrust forces generates on pipes during large earthquakes. However, the results for a loading mass of 14 kg (Figure 10(b)) show that the displacement of the pipe in case C increased during shaking at an amplitude of 6 m/s^2. Figure 9(b) shows images of test models after shaking (amplitude = 8 m/s^2, loading mass = 14 kg). As for the gravel layer on the passive side, the shape of that gravel layer deformed more in case C than in case D. The thickness of the gravel layer apparently affected this deformation. Increasing the thickness of this gravel layer may reduce the compressive stress on the gravel layer. Therefore, the layout of the gravel layer on the passive side of a pipe is important for pipeline stability.

4.3 Effects of gravel on the active side of a pipe

Gravel on the active side of the pipe is expected to reduce the movement of the pipe in the trench. The role of gravel on the active side is confirmed by the results of cases B, C and D. Figure 12(a) shows the acceleration of the pipe and the model ground during shaking (amplitude = 8 m/s^2, loading mass = 7 kg). Note that the acceleration shows a negative value if the acceleration generates toward the active side. Case C shows no data due to a measurement fault. The responses in case B with gravel on the active side showed no phase difference between the pipe and the ground, whereas the responses in case D without gravel on the active side showed a slight phase lag between the pipe and the model ground. Figure 12(b)

shows an enlarged view of pipe displacement during shaking (amplitude = 8 m/s^2, loading mass = 7 kg). The average amplitude of displacement between 30 and 40 s was 0.03 in case D but 0.01 in cases B and C. Although the amplitude of pipe displacement in case D was the largest, the total lateral displacement in case D after shaking was the same as in cases B and C, as shown in Figure 10(a). These test results indicate that gravel on the active side provides no thrust restraint effect.

4.4 Effectiveness of gravel backfill in uplift mitigation

As mentioned in subsection 3.2, the pipe without gravel (case A) moved obliquely. Mitigating the uplift is important for the stability of the pipe because uplift also causes pipe damage (e.g., joint separation). The effect of gravel in mitigating pipe uplift was confirmed by the test results.

Figure 13 shows the relationships between the lateral and upward components of pipe displacement. Pipe displacement measurements were obtained from photos and normalised by the outer diameter of the pipe. The upward displacement in cases A and C increased drastically with increasing lateral displacement. Furthermore, the relationship between lateral and upward displacement in case C was similar to that in case A. On the other hand, the pipes in cases B and D moved laterally while hardly uplifting. These differences in pipe behaviour were caused by the differences in gravel layout; gravel in cases B and D covered the upper quarter of the pipe on the passive side, while gravel in cases A and C did not. Some studies have assessed the effectiveness of gravel above a pipe in mitigating uplift. Ling *et al*. (2003) proposed a design procedure for mitigating pipe uplift based on test results and pointed out that the deadweight and stiffness of the gravel unit above a pipe, confined by geosynthetics, were important in mitigating pipe uplift in liquefied ground. The test results indicate that gravel above the pipe might suppress pipe uplift associated with lateral displacement.

5. Conclusions

In this study, four shaking table tests were conducted on the buried pipes under a 30 g simulated gravitation field for the purpose of evaluating effective layouts of gravel backfill as a thrust restraint under earthquake conditions. The main conclusions are as follows.

1) Under the typical thrust force magnitudes, the displacement of a pipe backfilled without gravel increased drastically beyond the allowable value during shaking, whereas that of a pipe with gravel remained within the allowable value even under the large earthquake conditions. These results revealed that gravel backfill works effectively as a thrust restraint against typical thrust force generated on pipes during earthquakes.

2) Under large thrust force magnitudes, the pipe moved substantially when the gravel layer extended only to the spring line of the pipe. On the other hand, the pipe remained within the allowable displacement when the gravel layer on the passive side extended to the top of the pipe, even if there was no gravel layer on the active side of the pipe.

3) The amplitude of pipe displacement during shaking increased when no gravel was placed on the active side of the pipe. However, the amplitude of the pipe displacement barely affected the total lateral displacement of the pipe. Therefore, gravel on the active side produced no meaningful thrust restraint effect.

4) Gravel on the upper half of the passive side of the pipe suppressed pipe displacement not only laterally but also upwards.

The above conclusions indicate that gravel is required on the passive side from the bottom to the top of the pipe. Therefore, a gravel layer on the passive side from the bottom to the top of the pipe (case D) is the best layout for thrust restraint among the four test conditions. The layout of gravel on the passive side of the pipe is crucial in mitigating lateral displacement at pipe bends.

As explained in subsection 2.2, the particle of gravel was too large to meet a requirement for the scaling effect. The test results may show an overestimation of the gravel layer effectiveness because of the large size of gravel. Further experimental studies are required to evaluate the effectiveness of gravel.

Acknowledgements

This work was supported by JSPS KAKENHI Grant Number 17H01495. The authors thank Dr A. Izumi for valuable suggestions for the experiments. The authors also acknowledge the valuable support of Tokyo Soil Research Co., Ltd.

References

American Water Works Association (2013) M45 Fiberglass Pipe Design, Third Edition. American Water Works Association, Denver, USA, pp. 87–98.

Audibert JME and Nyman KJ (1977) Soil restraint against horizontal motion of pipes. Journal of the Geotechnical Engineering Division **103(10)**: 1119–1142.

Cheong TP, Soga K and Robert DJ (2011) 3D FE analyses of buried pipeline with elbows subjected to lateral loading. Journal of Geotechnical and Geoenvironmental Engineering, **137(10)**: 939–948.

Daiyan N, Kenny S, Phillips R and Popescu R (2011) Investigating pipeline–soil interaction under axial–lateral relative movements in sand. Canadian Geotechnical Journal **48 (11)**: 1683–1695.

Fujita N, Mohri Y and Kishida T (2007) Behavior of curved pipeline formed with flexible joints subjected to internal pressure. Transactions of JSIDRE **75(2)**: 27–34 (in Japanese).

Harumoto T, Miyata T, Ariyoshi M, Mohri Y, Itani Y and Kawabata T (2015) Pipe behaviour in liquefied ground –seismic damage to the main agricultural pipeline in the Kumado river region- [Translated from Japanese.]. In *Proceedings of the 72th Regional Conference of JSIDRE Kyoto Branch*, JSIDRE, Otsu, Japan, pp. 210–211 (in Japanese).

Hsu TW (1993) Rate effect on lateral soil restraint of pipelines. Soils and Foundations **33(4)**: 159–169.

Huang D, Tang A and Darli CM (2020) Pipe-soil interaction at pipe bend under seismic load. Journal of Pipeline Systems Engineering and Practice **11(3)**: 04020023.

Itani Y, Fujita N, Ariyoshi M, Mohri Y and Kawabata T (2016) Dynamic behavior of flexibly jointed pipeline with a bend in liquefied ground. IDRE Journal **84(1)**: I_1-I_8 (in Japanese).

Kawabata T, Mohri Y and Ling HI (2002) Earth pressure distribution for buried pipe bend subjected to internal pressure. In *Proceedings of Pipeline Division Specialty Conference 2002*, ASCE, Cleveland, US, CD-ROM.

Klinkvort RT, Black JA, Bayton SM, Haigh SK, Madabhushi GSP, Blanc M, Thorel L, Zania V, Bienen B and Gaudin C (2018) A review of modelling effects in centrifuge monopile testing in

sand. In *Proceedings of the 9th International Conference on Physical Modelling in Geotechnics*, ISSMGE, London, UK, pp. 719–724.

Kouretzis GP, Sheng D and Sloan SW (2013) Sand–pipeline–trench lateral interaction effects for shallow buried pipelines. Computers and Geotechnics **54**: 53–59.

Ling HI, Mohri Y, Kawabata T, Liu H, Burke C and Sun L (2003) Centrifugal modeling of seismic behavior of large-diameter pipe in liquefiable soil. Journal of Geotechnical and Geoenvironmental Engineering **129(12)**: 1092–1101.

Ministry of Agriculture, Forestry and Fisheries of Japan (2009) Planning and Design Criteria of Land Improvement Project (Pipeline) [Translated from Japanese], JSIDRE, Shinbashi, Japan, pp. 387–409 (in Japanese).

Nozu A and Iai S (2001) Indicator of earthquake motion for immediate damage estimation for a quay wall [Translated from Japanese.]. In *Proceedings of the 28th Regional Conference of JSCE Kanto Branch*, JSCE, Maebashi, Japan, pp. 18–19 (in Japanese).

Ohta Y, Sawada Y, Kawamura M, Ono K and Kawabata T (2019) Shaking table tests for buried pipe bends with thrust restraints using geogrid and gravel in liquefied ground. In *Proceedings of the 29th (2019) International Ocean and Polar Engineering Conference*, ISOPE, Honolulu, US, pp. 2373–2377.

Ohta Y, Sawada Y, Ono K, Ling HI and Kawabata T (2018-a) Model experiments on influence of the bending angles on lateral resistance acting on buried pipe bends. In *Proceedings of the 28th (2018) International Ocean and Polar Engineering Conference*, ISOPE, Sapporo, Japan, pp. 589–593.

Ohta Y, Sawada Y, Ono K, Kawamura M and Kawabata T (2018-b) Effects of shape dimensions of the lightweight thrust restraint method for buried pipe bend on additional lateral resistance. Geosynthetics Engineering Journal **33**: 55–60 (in Japanese).

Ono K, Minaka US and Okamura M (2019) Dynamic centrifuge tests on dissipation effects of excess pore water pressure by gravel drains. Journal of Japan Association for Earthquake Engineering **19(6)**: 6_68-6_75 (in Japanese).

Ono K, Yokota Y, Sawada Y and Kawabata T (2016) Lateral loading test for buried pipe under different hydraulic gradient. In *Proceedings of the 26th (2016) International Ocean and Polar Engineering Conference*, ISOPE, Rhodes, Greece, pp. 664–669.

Palmer MC, O'Rourke TD, Olson NA, Abdoun T, Ha D and O'Rourke MJ (2009) Tactile pressure sensors for soil-structure interaction assessment. Journal of Geotechnical and Geoenvironmental Engineering **135(11)**: 1638–1645.

Roy K, Hawlader B, Kenny S and Moore I (2018) Lateral resistance of pipes and strip anchors buried in dense sand. Canadian Geotechnical Journal **55(12)**: 1812–1823.

Trautmann CH and O'Rourke TD (1985) Lateral force-displacement response of buried pipe. Journal of Geotechnical Engineering **111(9)**: 1077–1092.

Yumsiri S and Soga K (2006) DEM analysis of soil-pipeline interaction in sand under lateral and upward movements at deep embedment. Geotechnical Engineering Journal of the SEAGS and AGSSEA **37**: 83–94.

Figure captions

Figure 1. Thrust force at a bend in a pressure pipeline
Figure 2. Test conditions
Figure 3. Test container
Figure 4. Loading system
Figure 5. Grain size distribution
Figure 6. Results of the cyclic undrained triaxial tests
Figure 7. Acceleration responses of the shaking table
Figure 8. Response of excess pore water pressure ratio at model ground
Figure 9. Images of test models after shaking at the amplitude of 8.0 m/s^2
Figure 10. Normalised lateral displacement of the pipe
Figure 11. Flexible joint (Itani *et al*., 2016)
Figure 12. Responses of pipes buried with gravel
Figure 13. Relationship between lateral and upward displacement of the pipe

Table 1. Scaling laws

Quantities	Model/Prototype
Acceleration	n
Length	$1/n$
Force	$1/n^2$
Time (inertia)	$1/n$
Time (permeability)	$1/n$

Table 2. Calculated PSI values

	Maximum acceleration (m/s^2)	PSI value ($cm/s^{0.5}$)	Observation point
Shaking table tests	2.0 4.0 6.0 8.0	24 66 103 133	
The 2011 off the Pacific coast of Tohoku Earthquake	NS: 3.8 EW: 4.0 UD: 3.5	NS: 130 EW: 161 UD: 37	Shinmachi, Oketani cho, Miyagi prefecture, Japan

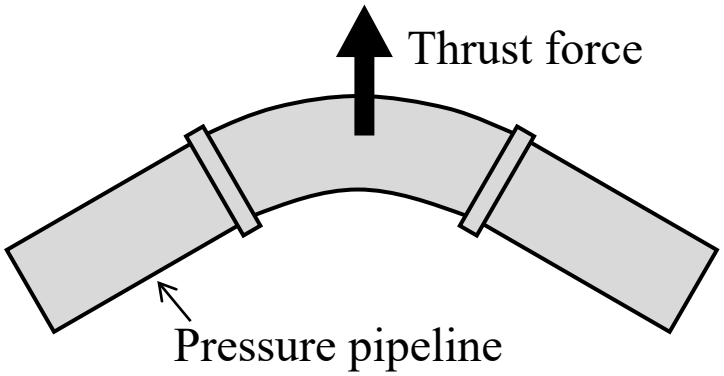

(a) Plan view

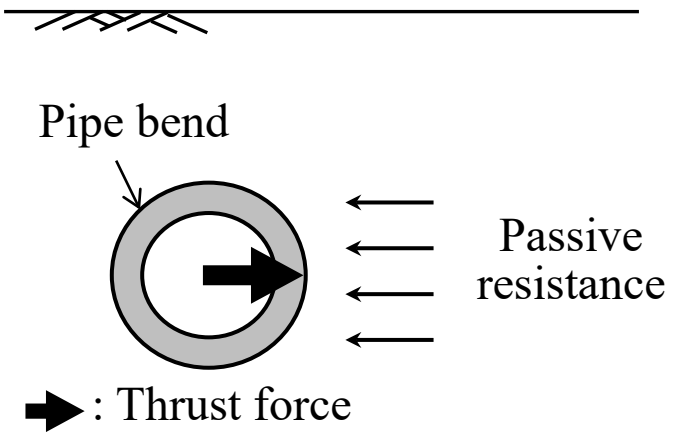

(b) Cross-sectional view

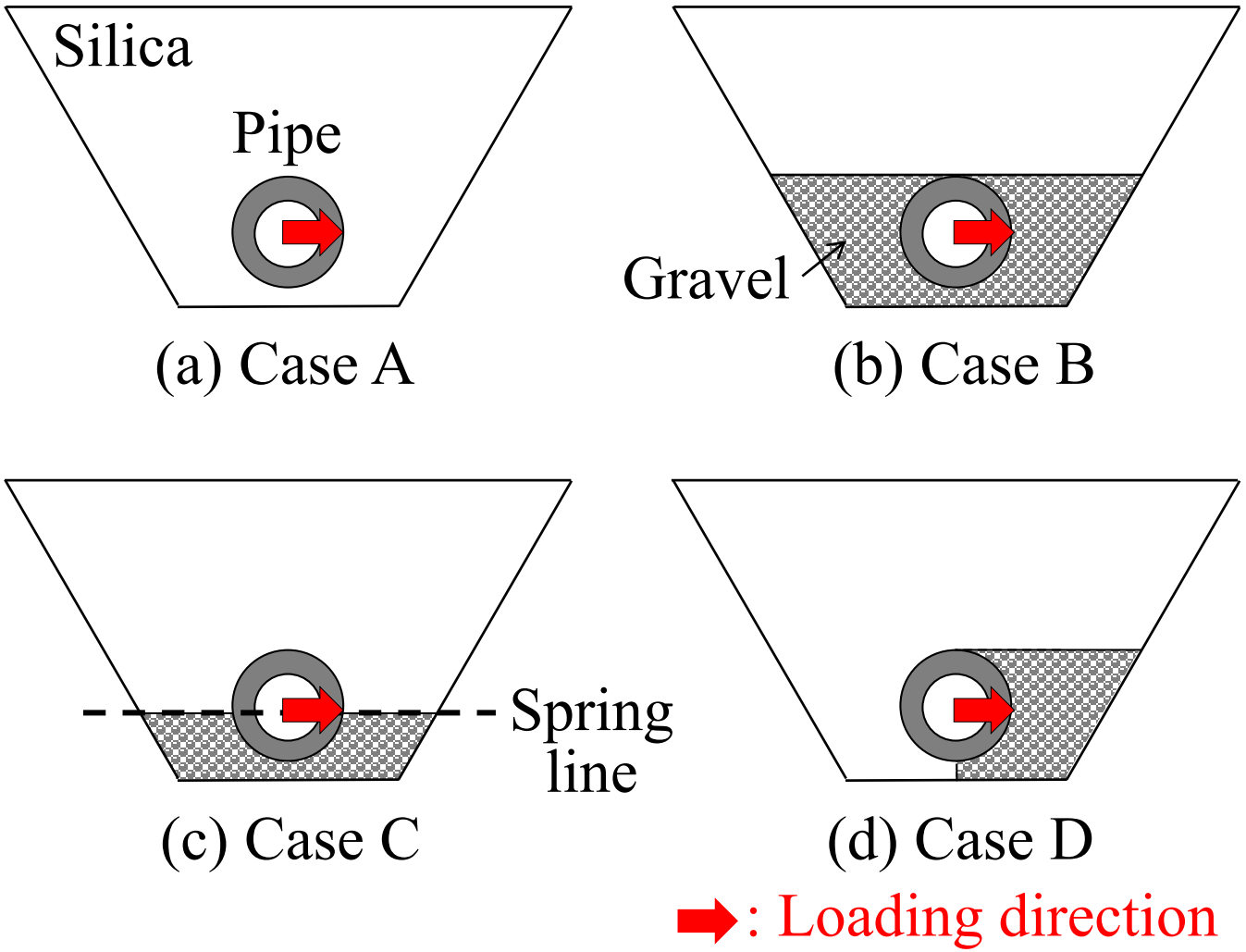
Silica
Pipe
(a) Case A
Gravel
(b) Case B
Spring line
(c) Case C
(d) Case D
: Loading direction

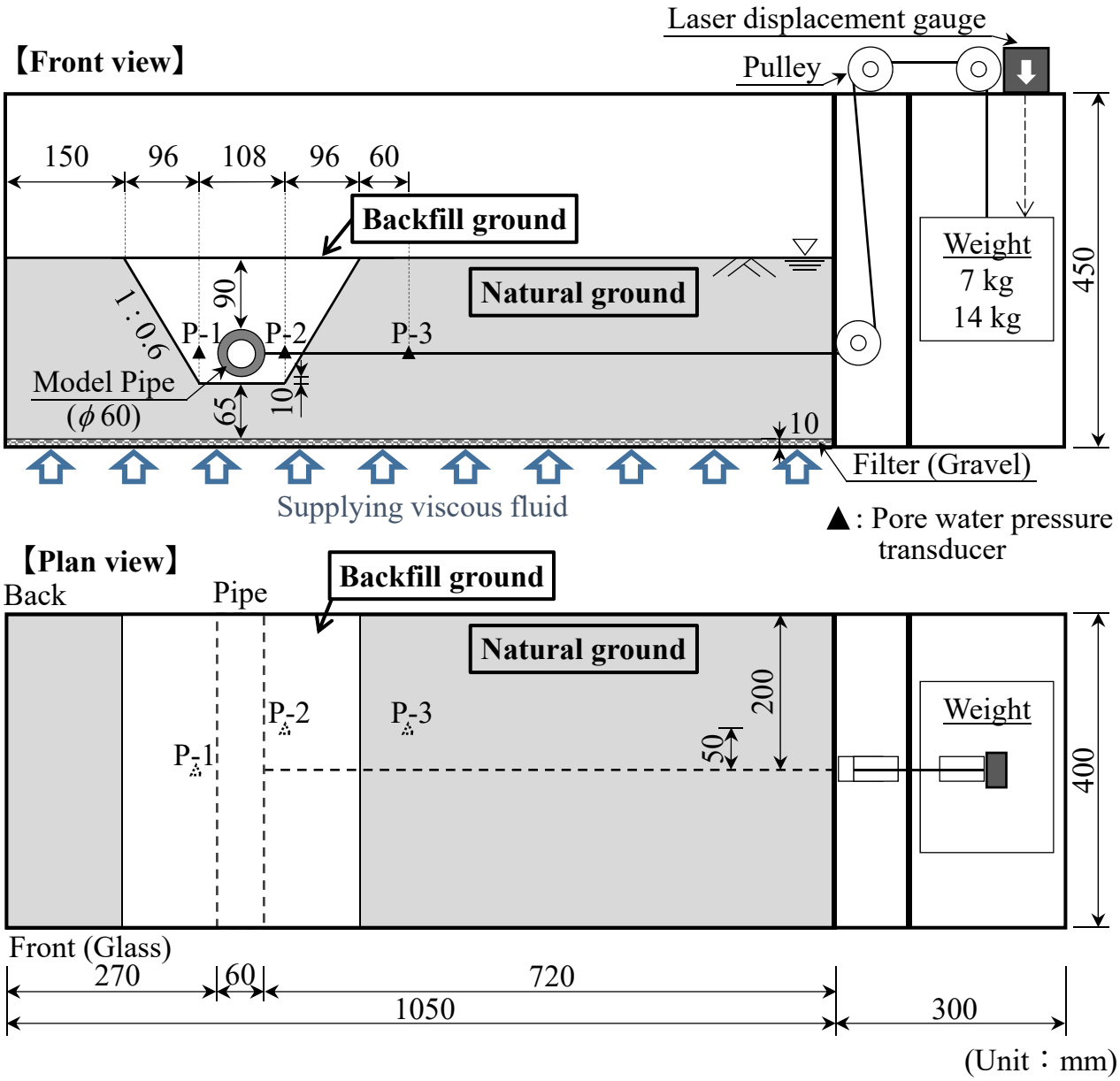
【Front view】
Laser displacement gauge
Pulley
150
96
108
96
60
Backfill ground
Natural ground
Weight
7 kg
14 kg
450
90
1 : 0.6
P-1
P-2
P-3
Model Pipe
(ϕ 60)
65
10
10
Filter (Gravel)
Supplying viscous fluid
▲: Pore water pressure transducer
【Plan view】
Back
Pipe
Backfill ground
Natural ground
P-1
P-2
P-3
200
50
Weight
400
Front (Glass)
270
60
720
1050
300
(Unit：mm)

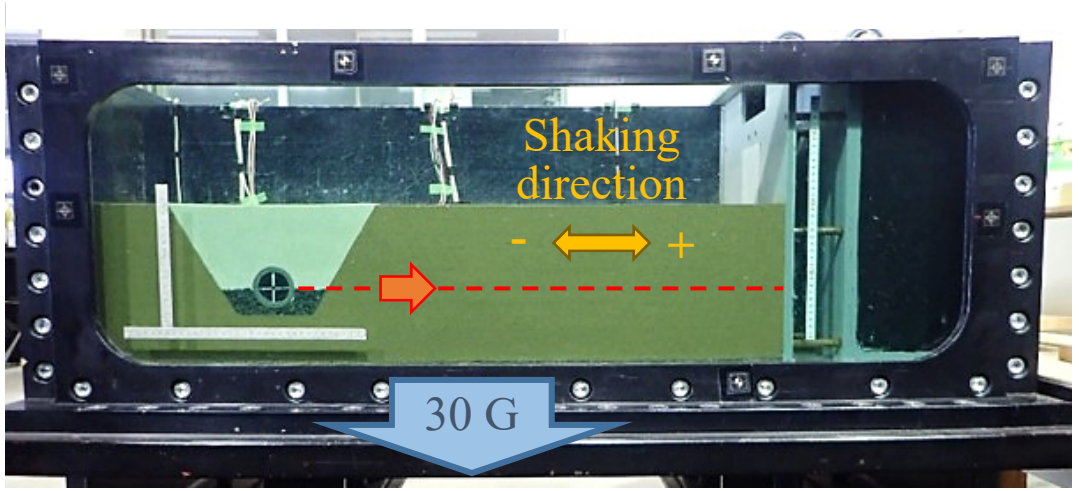

(a) Test container

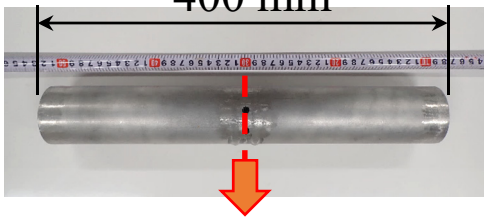

(b) Model pipe

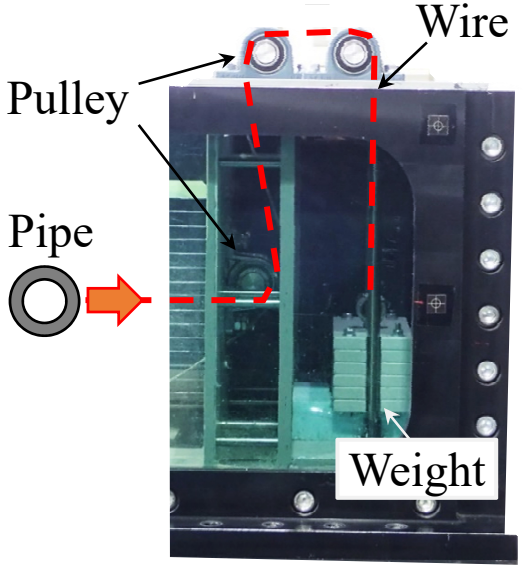

(c) Loading system

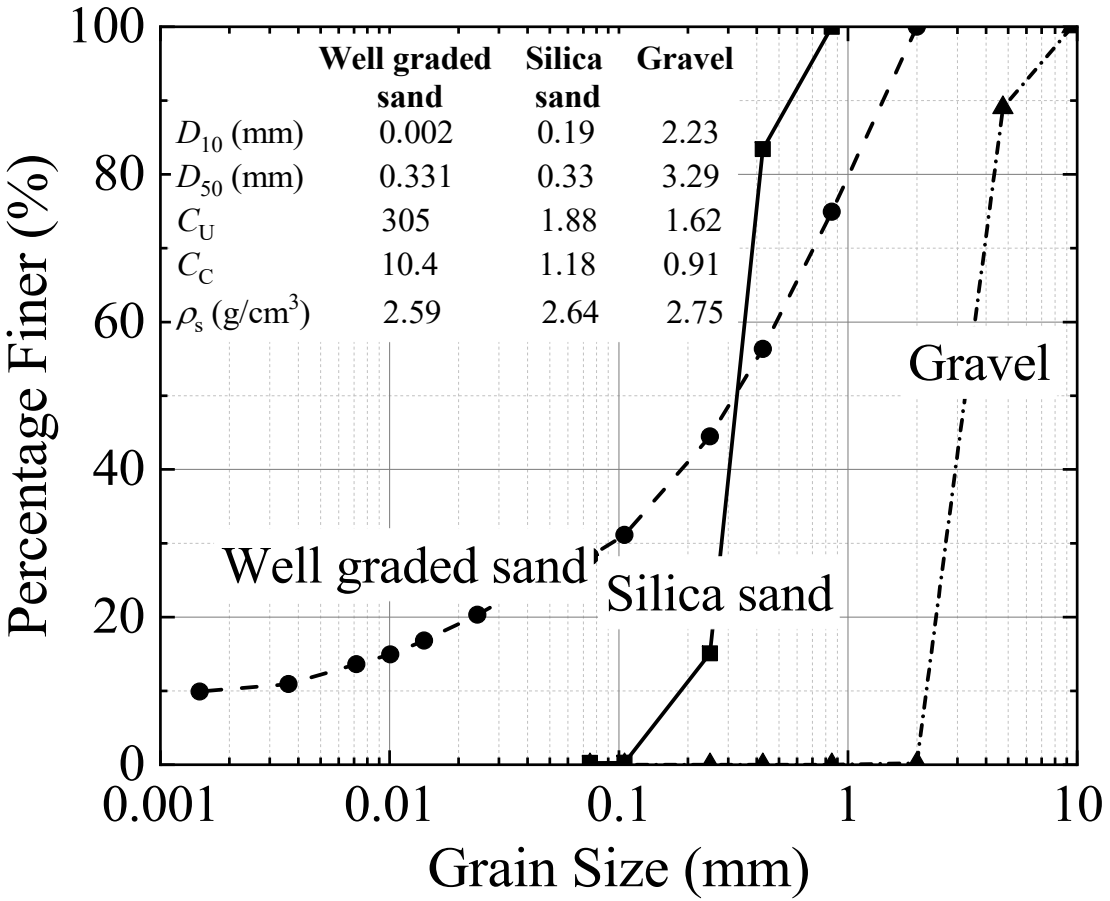
Well graded sand
Silica sand
Gravel
D_{10} (mm) 0.002 0.19 2.23
D_{50} (mm) 0.331 0.33 3.29
C_U 305 1.88 1.62
C_C 10.4 1.18 0.91
ρ_s (g/cm^3) 2.59 2.64 2.75
Well graded sand
Silica sand
Gravel
Percentage Finer (%)
Grain Size (mm)
0
20
40
60
80
100
0.001
0.01
0.1
1
10

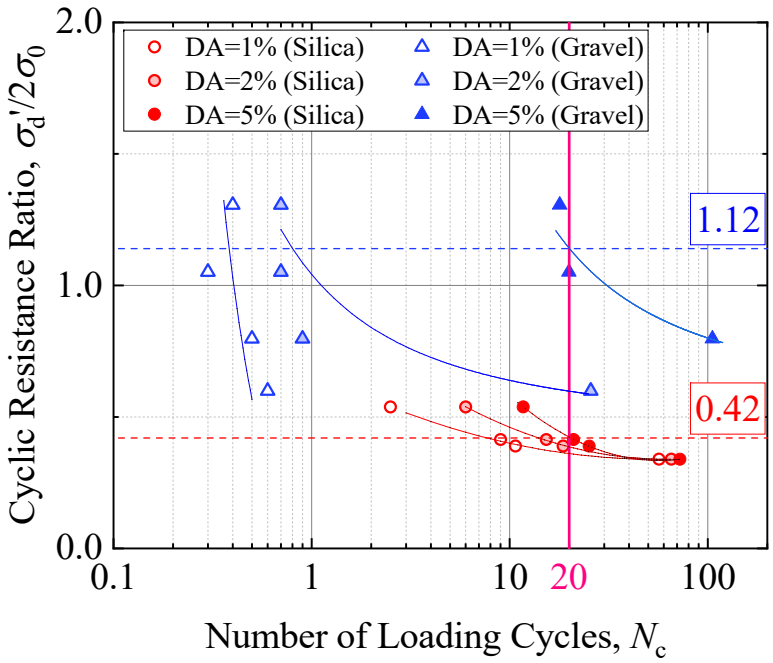

(a) Relationship between cyclic stress ratio and number of loading

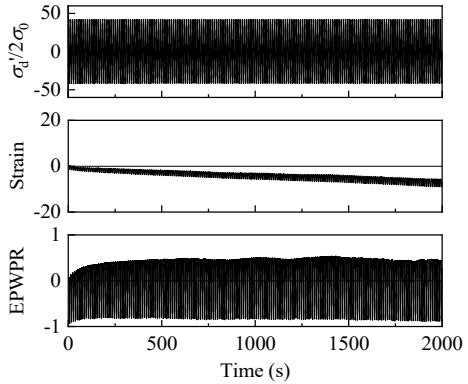

(b) Gravel

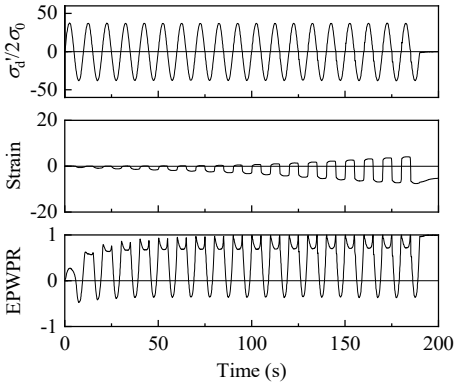

(c) Silica sand

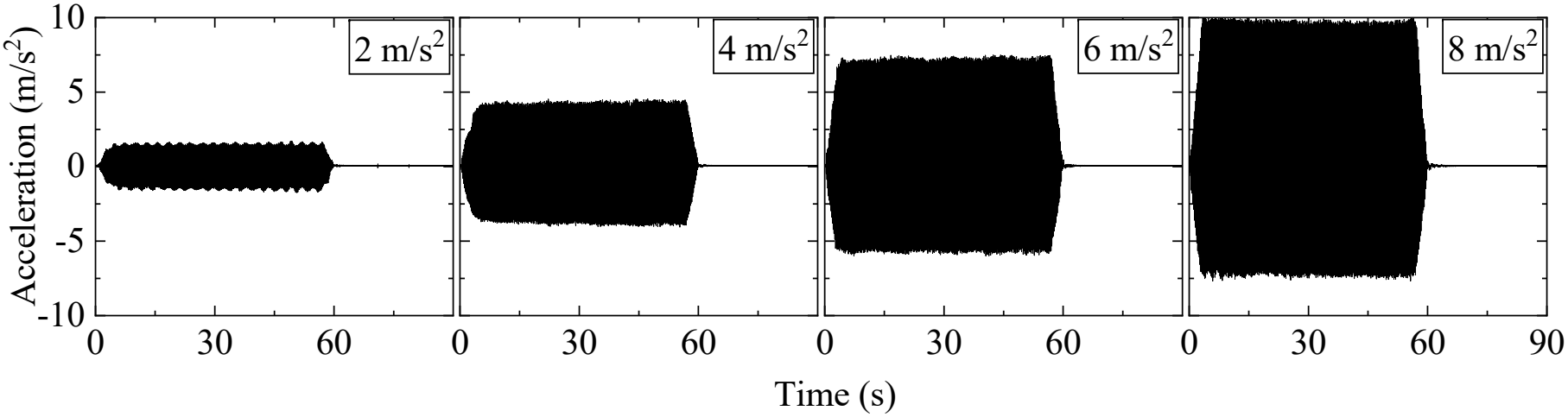
2 m/s2
4 m/s2
6 m/s2
8 m/s2
Acceleration (m/s2)
10
5
0
-5
-10
0
30
60
90
Time (s)

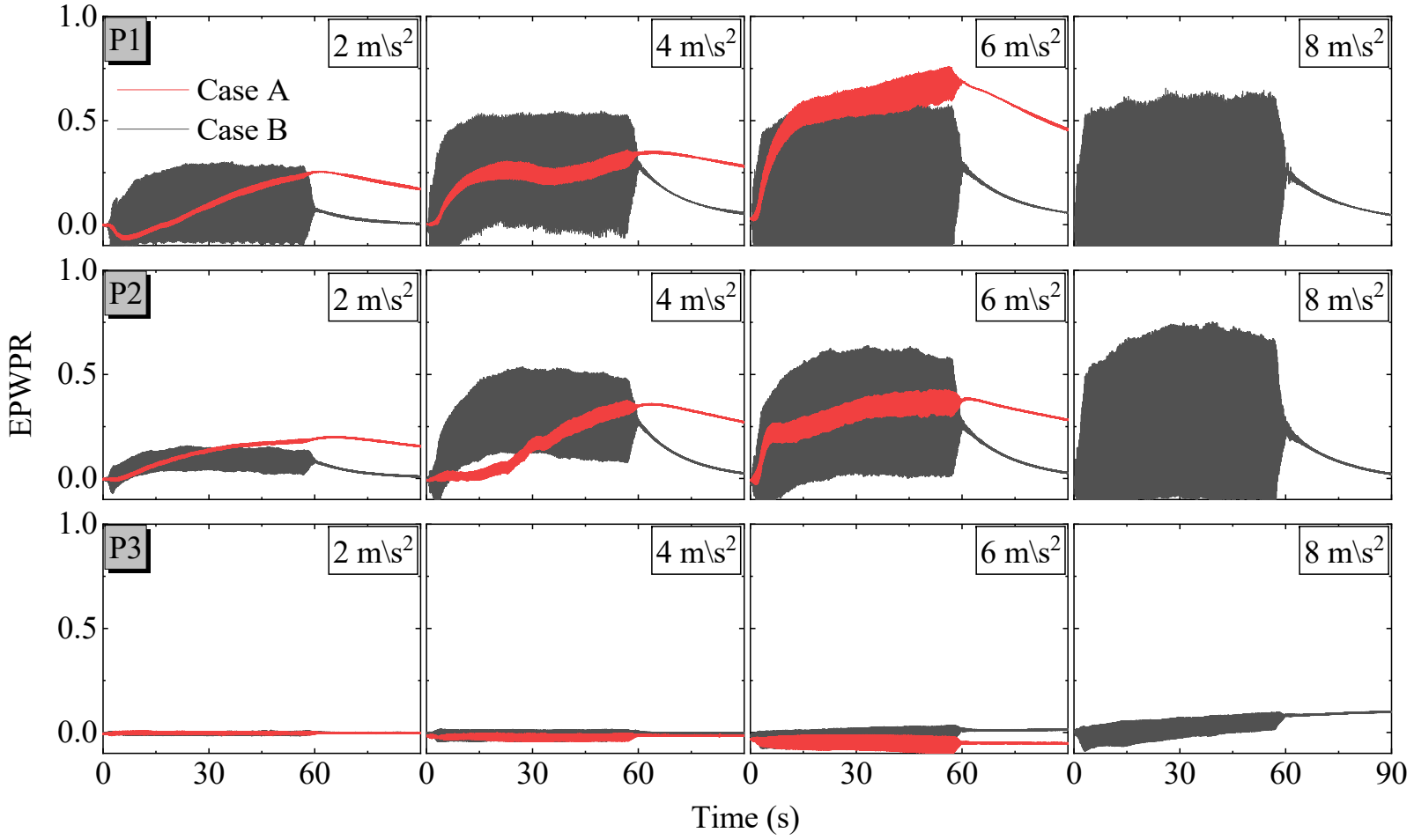
P1
P2
P3
Case A
Case B
2 m\s2
4 m\s2
6 m\s2
8 m\s2
EPWPR
1.0
0.5
0.0
0
30
60
90
Time (s)

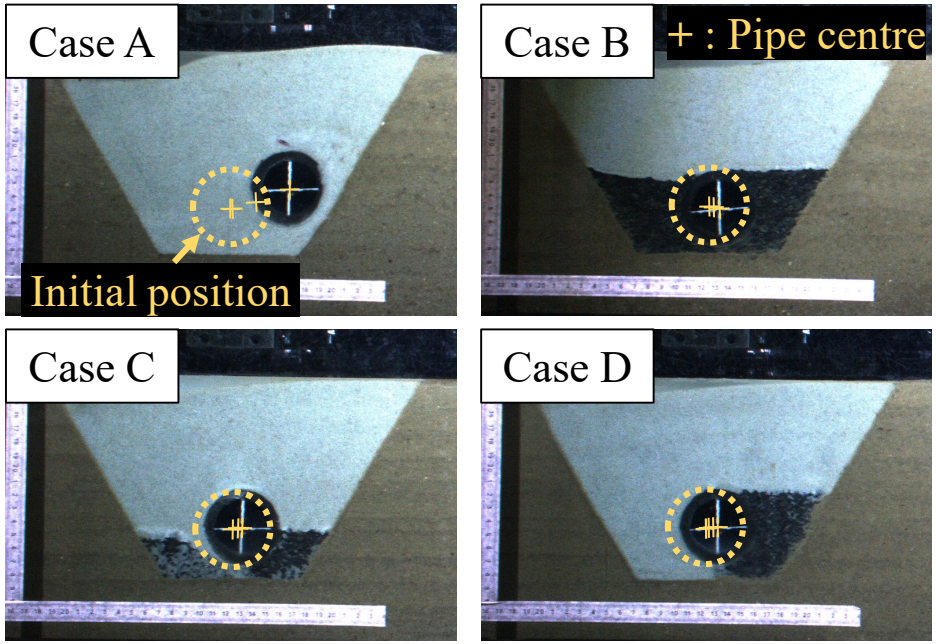

(a) Loading mass of 7 kg

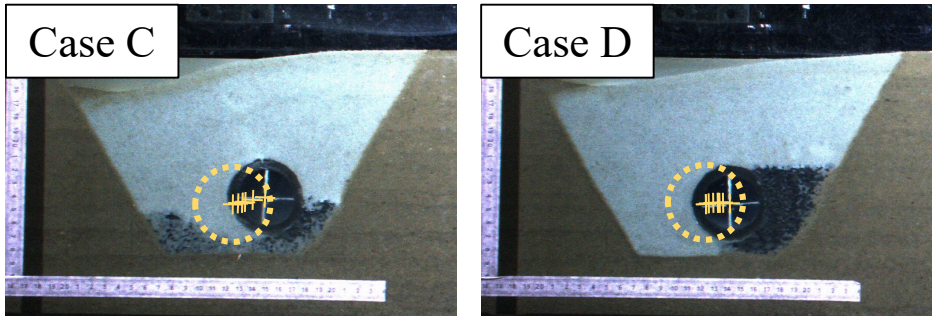

(b) Loading mass of 14 kg

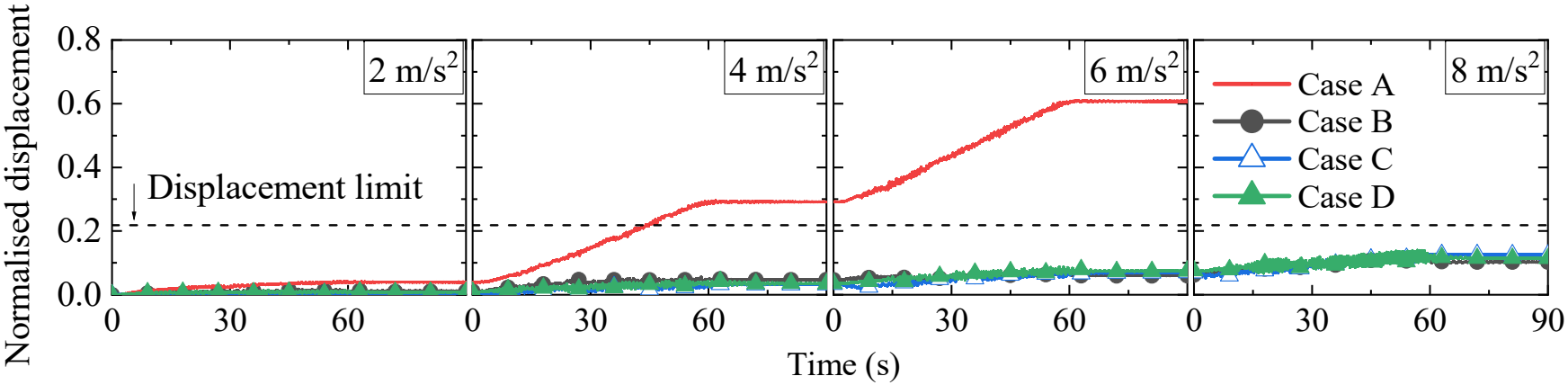

(a) Loading mass of 7 kg

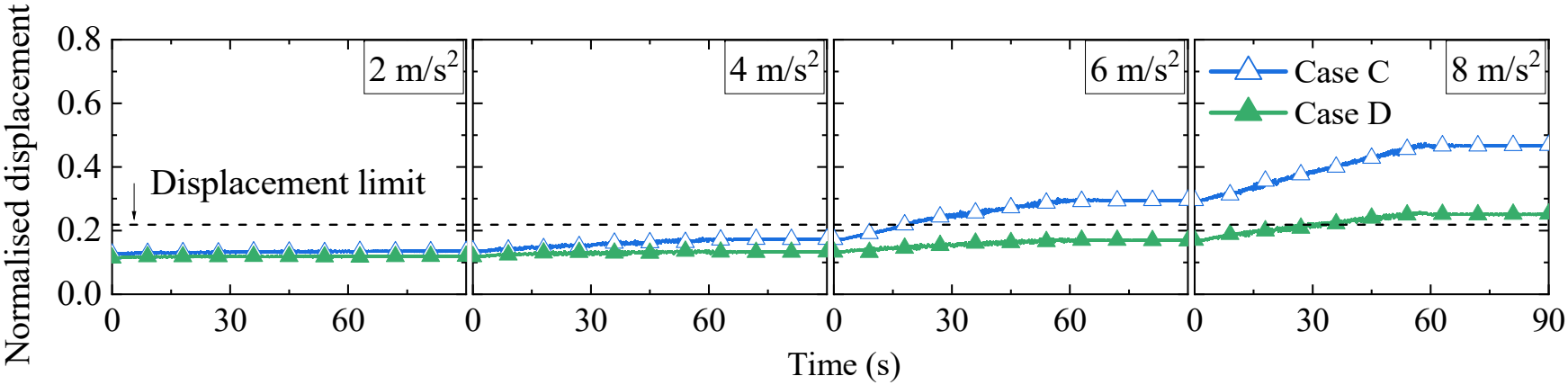

(b) Loading mass of 14 kg

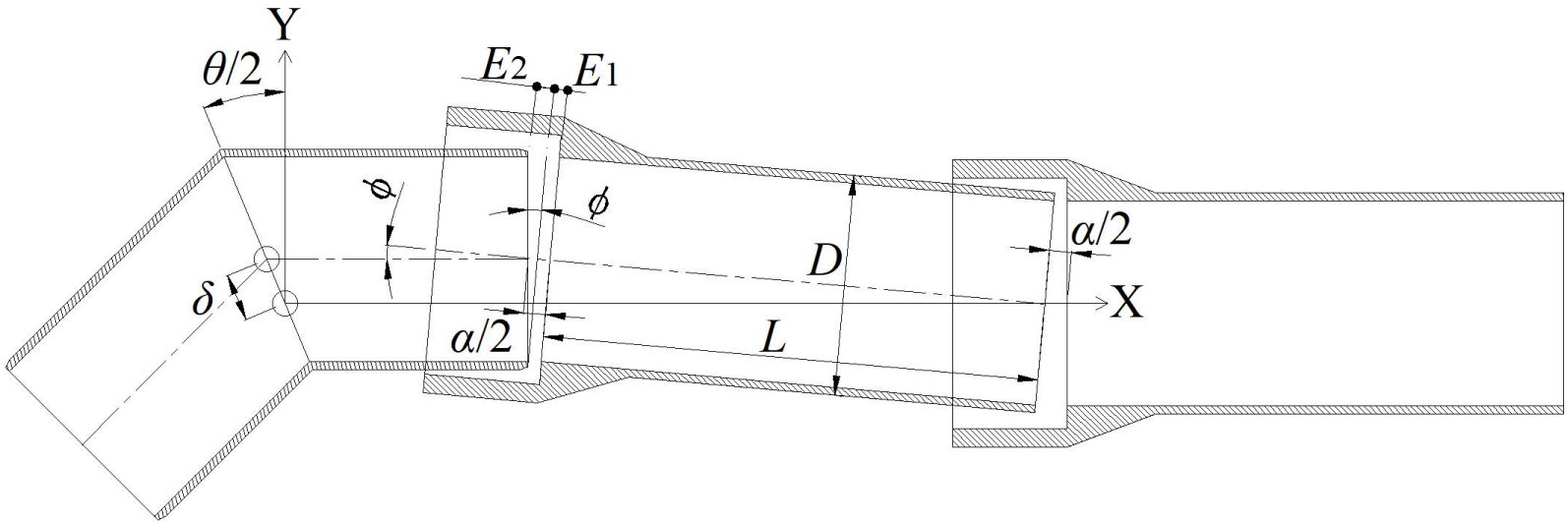
Y
θ/2
E2
E1
ϕ
ϕ
δ
D
α/2
X
α/2
L

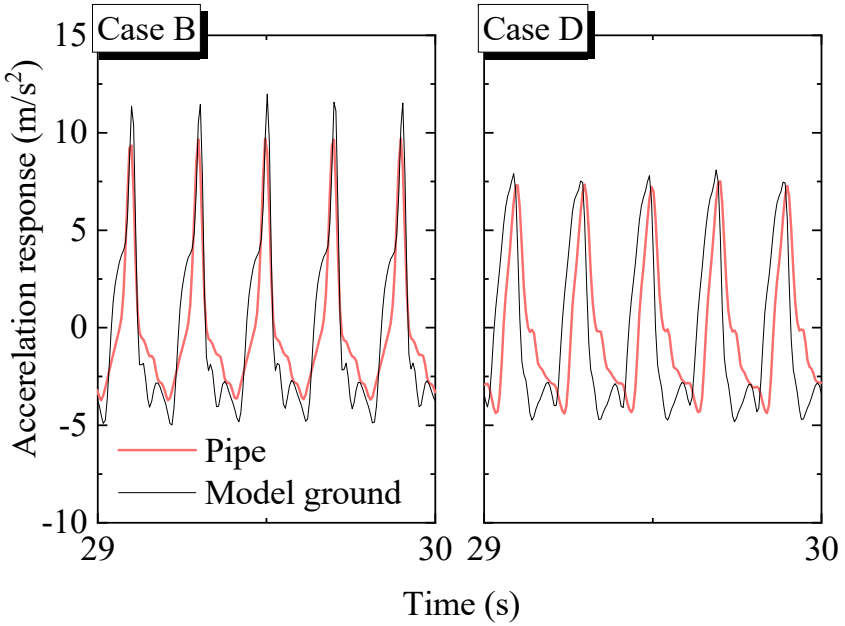

(a) Acceleration response at 8 m/s^2 shaking
(Loading weight with 7 kg)

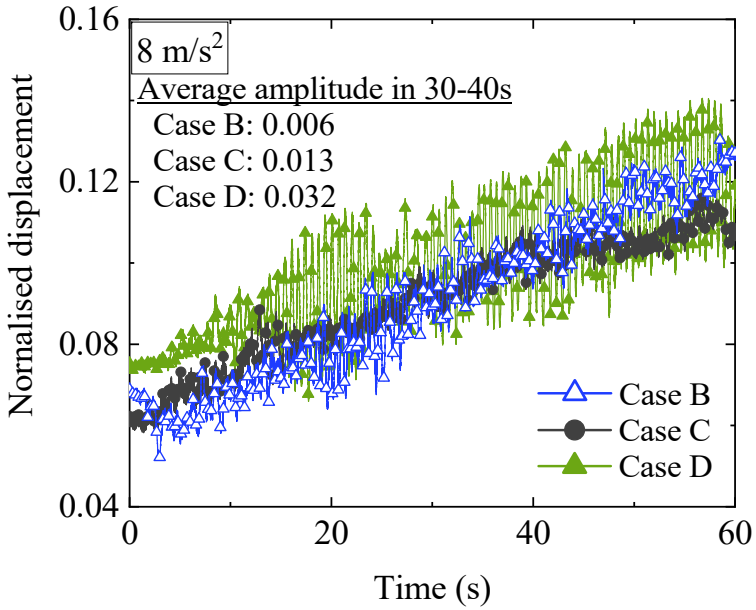

(b) Displacement of the pipe at 8 m/s^2 shaking
(Loading weight with 7 kg)

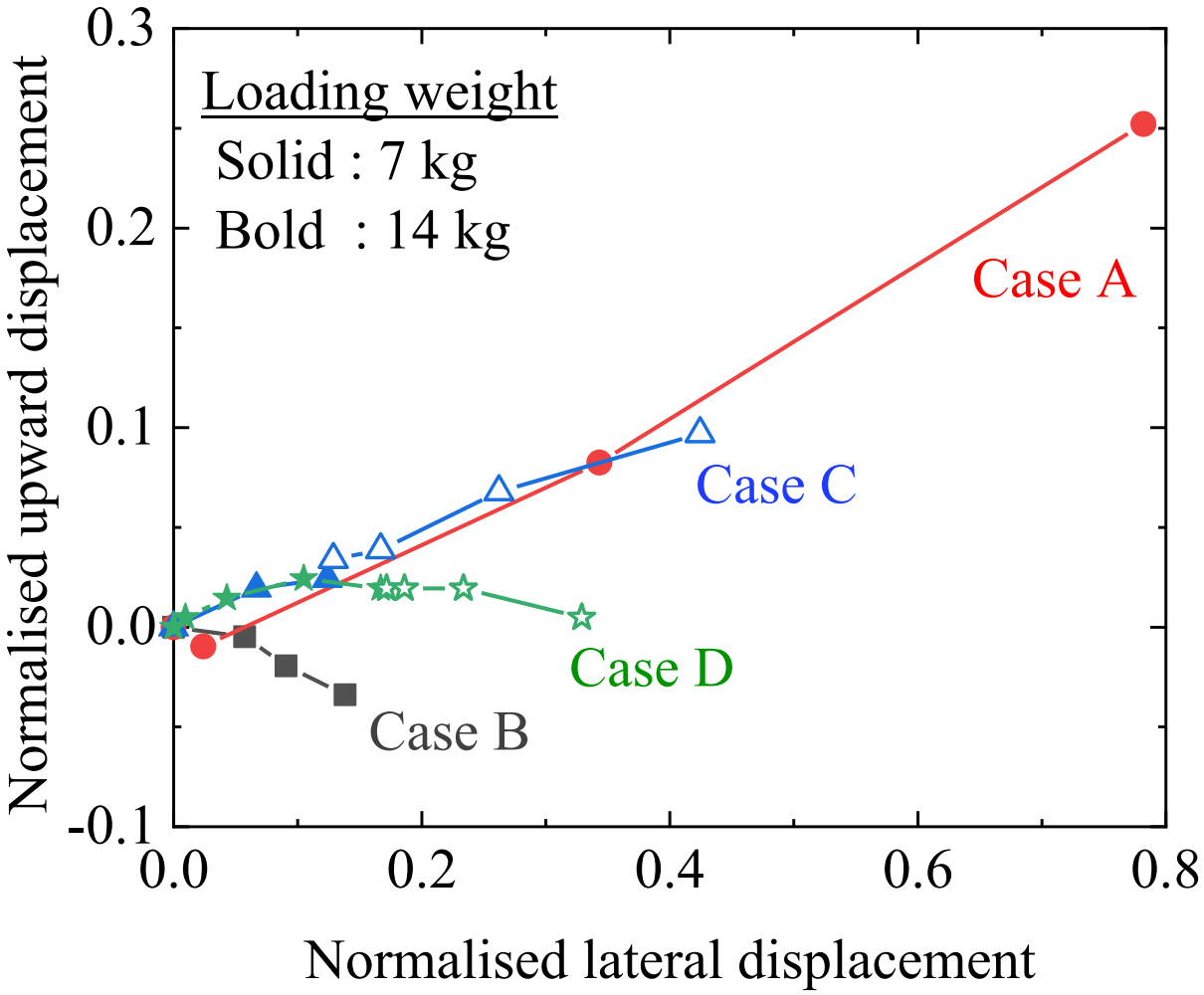
Loading weight
Solid : 7 kg
Bold : 14 kg
Case A
Case C
Case D
Case B
Normalised upward displacement
Normalised lateral displacement
0.3
0.2
0.1
0.0
-0.1
0.0
0.2
0.4
0.6
0.8